Computers, Environment and Urban Systems 48 (2014) 86–98

Contents lists available at ScienceDirect

Computers, Environment and Urban Systems

journal homepage: www.elsevier.com/locate/compenvurbsys

Land use patterns, temperature distribution, and potential heat stress risk – The case study Berlin, Germany

Pierre-Adrien Dugord [a], Steffen Lauf [a,*], Christian Schuster [b], Birgit Kleinschmit [a]

[a] Technische Universität Berlin, Dept. of Landscape Architecture and Environmental Planning, Geoinformation in Environmental Planning Lab, Berlin, Germany
[b] Humboldt Universität zu Berlin, Dept. of Geography, Geoinformation Science Lab, Berlin, Germany

ARTICLE INFO

Article history:
Received 3 November 2013
Received in revised form 15 May 2014
Accepted 20 July 2014

Keywords:
Urban heat island
Land use patterns
Landscape metrics
Soil sealing
NDVI
Heat-stress risk
Vulnerability
Demographic change
Climate change
Berlin

ABSTRACT

In western societies, the combined effects of climate warming, proceeding urbanization, and demographic change (e.g. population aging) increase the risk of city populations to be subjected to heat-related stress. To provide a scientific fundament for city-wide and spatially explicit adaptation planning, urban heat distribution and the population at risk need to be studied at small spatial scale. This study pursued to (a) investigate the land surface temperature (LST) distribution with regard to underlying effects of urban land use patterns, and to (b) identify areas at potential risk towards heat stress based on temperatures distribution and demographic vulnerability. We used LST maps as derived from two Landsat thermal satellite images for 10 pm and 10 am at two subsequent summer days and examined land use patterns through land use types, landscape metrics, and structural parameters via statistical and GIS analysis. Using linear regressions we obtained the degree of soil sealing to be the best predictor of LST-variations. However, under certain conditions, NDVI, distance to city center and floor area ratio (FAR) were better predictors. Water bodies had beneficial effects at 10 am and inverse effects at 10 pm, vice versa for arable land. The cooling effects of green areas were more significant in the morning than in the evening. Residential uses were among the most heat affected land use types at 10 pm, with different intensities according to their density level. For the identification of risk areas at the building scale, we introduced a matrix to combine simulated air temperature with population age and density. Results showed higher potential risk in central inner-city areas of dense residential uses, in particular for areas with high amounts of elderly residents, and for two major residential building types. The identified building blocks of specific heat stress risk provide urban planners with useful information to mitigate adverse effects caused by future heat waves.

1. Introduction

In western societies, the combined effects of climate warming, proceeding urbanization, and demographic change (e.g. population aging) increase the risk of city populations to be subjected to heat-related stress (Gabriel & Endlicher, 2011; Harlan, Brazel, Prashad, Stefanov, & Larsen, 2006; Lauf, Haase, Hostert, Lakes, & Kleinschmit, 2012b). To provide a scientific fundament for city-wide and spatially explicit adaptation planning, urban heat distribution and the population at risk need to be studied at small spatial scale (Cao, Onishi, Chen, & Imura, 2010; Harlan, Declet-Barreto, Stefanov, & Petitti, 2013; Scherer et al., 2013).

Cities are characterized by increased air and surface temperatures as compared to their rural surroundings. This so called urban heat island (UHI) effect is caused by the specific urban structure, the set of physical features which can be described by land-use (LU) patterns and other structural indicators, such as the degree of surface sealing (Thinh, Arlt, Heber, Hennersdorf, & Lehmann, 2002). Artificial building materials increase the heat storage of the surface, and automotive combustion engines and pollution emissions further heat up air temperatures, while cooling effects through vegetation cover and air flow are reduced (Oke, 1982; Schwarz, Schlink, Franck, & Grossmann, 2012). Gill, Handley, Ennos, and Pauleit (2007) argue that there is not only one single heat island, but claim that several of them can be differentiated within a city, scattered in between areas with low temperatures. Accordingly, dense sealed and built-up areas such as inner-city residential areas are considerably warmer than large urban parks, which represent a potential source of cooling through evapotranspiration and fresh air generation (Bolund & Hunhammar, 1999; Gill et al., 2007). This cooling effect inside of green spaces compared to their surroundings is often referred to as the park cool island (PCI),

* Corresponding author.

http://dx.doi.org/10.1016/j.compenvurbsys.2014.07.005
0198-9715/

(Spronken-Smith & Oke, 1998 and Mathey et al., 2010; Spronken-Smith & Oke, 1999).

Several authors argue that there is a relationship between the UHI intensity, the city size, structural characteristics (including LU patterns) and population concentration (Eliasson & Svensson, 2003; Gill et al., 2007; Li et al., 2011). In this context it is widely recognized that the greatest importance of micro-climatic regulation is offered by vegetation at different spatial scales (Lauf, Haase, & Kleinschmit, 2014; Reid et al., 2009). However, there is a lack of knowledge concerning the climatic effects of different LU types and LU patterns at different spatial scales (Cao et al., 2010; Chang, Ming-Huang, & Shyh-Dean, 2007; Mathey & Rößler, 2011; Patino & Duque, 2013).

Heat stress is considered to be a phenomenon induced by hot atmospheric conditions negatively affecting the energy balance of the human body and implying an increase of heat-related mortality and morbidity (Kovats & Hajat, 2008). Recent studies followed risk assessment concepts to quantify populations at risk of being objected by adverse climate change impacts (e.g. heat stress), in view of finding relevant adaptation measures (Birkmann et al., 2013; Depietri, Welle, & Renaud, 2013; Schneider et al., 2007). The wide and different use of risk and vulnerability concepts is challenging and requires a clear definition of the considered elements for a sound analysis (cf. Cutter, 1996; Gallopin, 2006). According to the definitions of heat –related risk of the IPCC we stress the key elements of a risk analysis, which are the hazard defining the probability that an element at risk (i.e. the urban population) is exposed to and the vulnerability defining the exposure and sensitivity of the population at risk (Scherer et al., 2013; Schneider et al., 2007). The exposure refers to the number and location of the population exposed to the (heat) impact, while sensitivity refers to the physiological condition of the exposed population (Birkmann et al., 2013; Johnson, Stanforth, Lulla, & Luber, 2012).

In the context of urban heat stress, the number of people exposed to heat impacts is expected to increase due to increasing urbanization (Zhang & Yeh, 2011). Also, in western societies, the population at risk may be further increased as a result from increased sensitivity due to population aging. Most studies on temperature an mortality relationships agree that the elderly are predominantly affected by heat stress, mainly due to their decreased ability to thermoregulate their body temperature and predispositions resulting from diseases like heart, circulation and respiratory diseases, diabetes mellitus, etc. (Oudin Åström, Bertil, & Joacim, 2011; Reid et al., 2009). Regarding young children as another age-specific sensitivity group (Kovats & Hajat, 2008), they are also expected to be more vulnerable due to their limited thermoregulation capacities, which has, however, not been clearly shown in mortality studies (Ishigami et al., 2008). Apart from age-distribution, population density represents another demographic factor that increase the exposure quantitatively and thus the vulnerability to be subjected to heat stress (Johnson et al., 2012; Romero-Lankao, Qin, & Dickinson, 2012; Scherer et al., 2013).

UHIs are likely to increase in intensity due to the process of climate change and the associated increase of extreme climatic events such as heat waves (Gabriel & Endlicher, 2011; Gill et al., 2007; Harlan et al., 2006; Kovats & Hajat, 2008). In combination with increasing urbanization rates and population aging, climatic change is regarded as major urban sustainability issue (Zhang & Yeh, 2011). For resilient urban planning in the prospect of future weather conditions and demographic change, knowledge concerning the climatic effects of different LU types and the distribution of vulnerable inhabitants at risk should be gained at different scales to support decision-makers (i.e. urban planners).

This study pursues two goals: First, to explore the drivers influencing the temperature distribution based on the LU patterns on different spatial scales, focusing on the relative influence of different types of green space; second, to identify sites of potential heat-stress risk in the city by relating the spatial distribution of temperatures and of vulnerable people at the block level.

2. Methods and materials

2.1. The study area

Berlin, the capital city of Germany, is located in the north-east of Germany, covers an area of 892 km^2 and is populated by 3,513,026 inhabitants (Amt für Statistik Berlin-Brandenburg, 2012). Berlin is characterized by a mainly flat topography. The climate is characterized by cold winters and warm summers. During 2000 and 2010, a daily mean temperature of 19.0 °C (SD = 3.2) was observed for the two warmest month, and several heat stress events are reported especially for 2006 and 2010 (Gabriel & Endlicher, 2011; Scherer et al., 2013; Appendix, Fig. A6). Regarding the LU patterns, Berlin is characterized by a significant amount of green infrastructures and water bodies. A relatively low building and population density outside the inner-city, many allotment gardens for private cultivation and recreation and a considerable amount of urban brownfields exist, despite the slight trend of population growth in the last decade. While some crucial local structural changes took place since the early 1990s (especially at the location of the former Berlin wall), the overall LU patterns remained relatively constant over the last decade (Lauf et al., 2014).

As illustrated in Fig. 1, Berlin consists of 45% water bodies and urban green spaces (forested and unforested, allotment gardens), almost 20% transport and infrastructural areas (streets and railways) and around 35% built-up areas (e.g. residential uses).

2.2. Effects of the land-use patterns on the temperature distribution

2.2.1. Land surface temperature

Several studies prove LST to be convenient for studying UHI on large scales since comprehensive distribution of measured air temperatures are hardly ever available (Kottmeier, Biegert, & Corsmeier, 2007; Li et al., 2011; Schwarz et al., 2012; Weng, Liu, & Lu, 2007). Accordingly, the term surface urban heat island (SUHI) is occasionally used instead of UHI (Li et al., 2011; Schwarz et al., 2012).

We applied Landsat-7 ETM+ LST data because of their high spatial resolution to enable the coupling with LU patterns information down to the level of individual building blocks (cf. Table 1; Patino & Duque, 2013). The small temporal interval between both datasets (12 h) enables to study the SUHI phenomenon, both in the morning and evening under comparable weather conditions (the air temperatures trend over the last decade is shown in the Appendix, Fig. A6).

Fig. 2 shows that at 10 am vegetated areas are obviously cooler than the built-up surroundings, agricultural areas, in contrast, reveal relatively high temperatures. At 10 pm increased LST are mostly concentrated in the inner city and agricultural areas are distinctively cooler.

2.2.2. Indicators describing the land-use patterns

We applied four different types of indicators to describe the LU patterns, namely LU types, landscape metrics, simple structural and aggregated structural indicators, and LU type indicators (cf. Table 2). The first three types were defined at the block-level, the aggregated ones at an intermediate spatial level between building blocks and administrative districts, the so-called LOR-level (official planning areas of the Berlin senate administration for sub-district

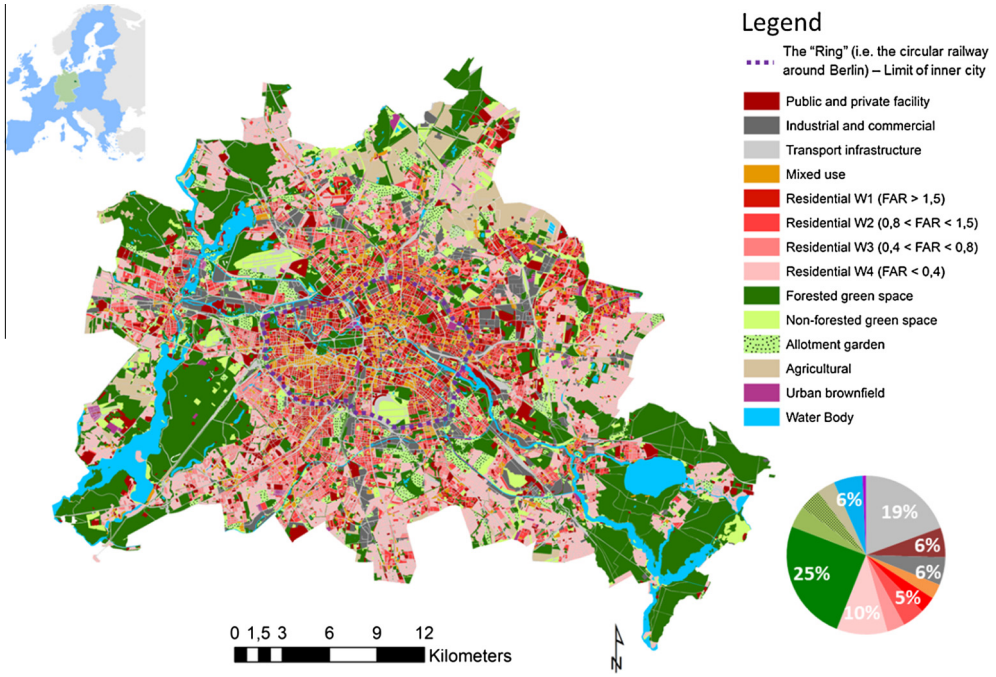

Fig. 1. The case study area of Berlin and its LU types with its relative proportions and floor area ratios (FAR); the dotted line represents the extend of the inner-city (bounded by the central circular railway).

Table 1
Overview of applied data within the study.

Data name	Origin of the data
Analysis of the effect of the urban pattern on the urban climate	
Land surface temperature (LST)	BSDUDE (2001–2013): Berlin Digital Environmental Atlas, (04.06) Surface Temperatures Day and Night (Edition 2001); Acquisition method: Landsat-7 ETM+; Spatial Resolution: 30 × 30 m Meteorological conditions measured at the Dahlem's Station of the Free University of Berlin: August 13, 2000, 10 pm; CET: Cloud cover = 0/8; wind velocity = 3.0 m/s; air temperature at 2 m altitude = 19.2 °C and August 147, 2000, 10 am; CET: Cloud cover = 1/8; wind velocity = 2.0 m/s; air temperature at 2 m altitude = 24.2 °C
Land-uses degree of soil sealing floor-area-ratio	BSDUDE (2001–2013): Berlin Digital Environmental Atlas, (06.01 and 06.02) Actual Use of Built-up Areas and Inventory of Green and Open Spaces (Edition 2002); Block Structure ISU50 (Scale 1:50 000), (Edition 2002)
NDVI	Calculation using Erdas Imagine 2011 from a Landsat 7 ETM + image (August 14, 2000)
Distance to city-center	Calculation using Arc10® based on LULC map; the TV Tower on the "Alexander Platz" was considered as the central point of the inner city
Landscape metrics	Calculation based on the LULC made with FRAGSTATS v.4 (Spatial Pattern Analysis Program for Categorical Maps)
Aggregated indicators at intermediate level	Calculation made with Arc10 based on the above mentioned parameters (see Table 2 for the calculation method)
Analysis of the potential heat stress risk	
Near ground air temperatures	BSDUDE (2001–2013): Berlin Digital Environmental Atlas, (04.10) Climate Model Berlin Analysis Maps (Edition 2009); Simulated Data-set (temperatures at 06 am and 10 pm, 0–5 meters above ground); using the FITNAH model (Flow over Irregular Terrain with Natural and Anthropogenic Heat), (e.g. Gross, 1993); CET: Cloud cover = 0/8; wind velocity = 0; humidity = 50%; Spatial resolution = 50 × 50 m; 2.5 meters above ground
City structure	BSDUDE (2001–2013): Berlin Digital Environmental Atlas, Block Structure ISU5 (Scale 1:5000), (Edition 2011)
Demographic data	(SOBB, 2013), Registered Inhabitants of primary residence on June 30, 2012 in statistical Blocks; Sorted across age groups, nationality, gender

administrative units). Berlin is structured in more than 30,000 single blocks and 447 LORs (BSDUDE, 2001–2013; Appendix, Fig. A3). Blocks exhibit a mean size of 0.06 km^2 (SD = 0.16 km^2) and a mean population of 131 (SD = 267 inh.) while LORs exhibit a mean size of 1.99 km^2 (SD = 3.04 km^2) and a mean population of 7500 inhabitants (SD = 1600 inh.).

As shown in Fig. 1, LU types are split into 14 classes based on the official classification of Berlin's master plan, combined with additional information on the use of other built-up areas and the inventory of green and open spaces (BSDUDE, 2001–2013). Landscape metrics, defined as quantitative indices to describe the spatial structure and pattern of the landscape (Herold, Scepan, & Clarke, 2002; Li et al., 2011; McGarigal, Cushman, & Ene, 2012; Weng, Lub, & Schubringa, 2004), were applied on the basis of these classes. We focused on diversity, area and edges, shape and aggregation metrics (cf. Table 1) which can be computed either at landscape or class level (McGarigal et al., 2012). For this study, landscape metrics were computed with the software FRAGSTATS v.4 via moving window (i.e. round local kernel with a radius of 100 m) where the class or landscape metrics of each window is returned to the focal cell representing the local neighborhood (McGarigal et al., 2012). The grid-based results were then

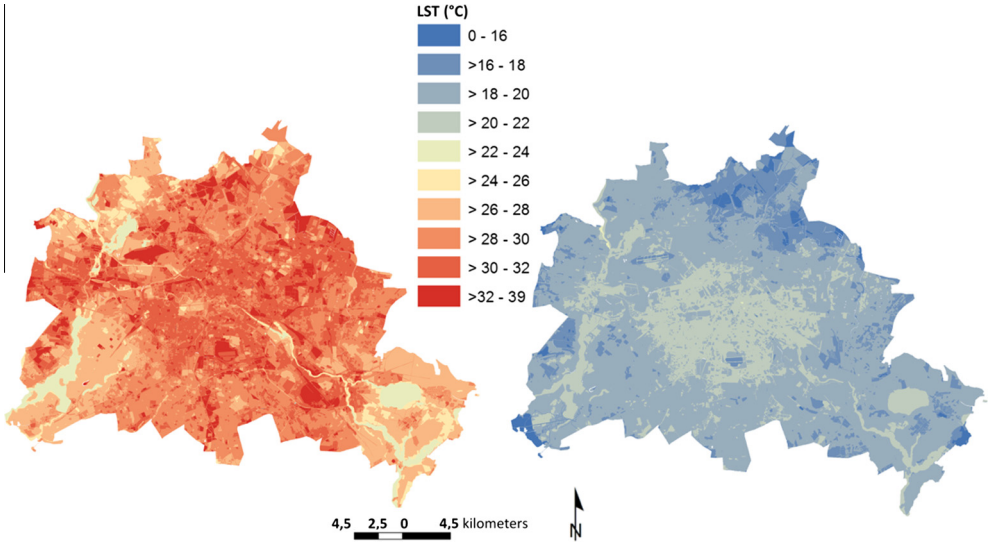

Fig. 2. Land surface temperature (LST) in °C in August for Berlin at 10 am (left) and 10 pm (right).

Table 2
Applied LU pattern indicators, (a) landscape pattern 170 metrics, after McGarigal et al. (2012), and (b) structural indicators at block and aggregated LOR-level.

Indicators	Level	Description
Landscape metrics		
Diversity metrics		
Simpson's evenness index (SIEI)	Landscape	SIEI expresses maximum evenness when the distribution of area patch types is even ecology and increase with landscape diversity
Simpson's diversity index (SIDI)	Landscape	SIDI is a popular measure of diversity in community ecology and increases with landscape diversity
Area and edge metrics		
Percentage of landscape area (PLAND)	Class	PLAND quantifies the proportional abundance of each patch type in the landscape
Edge density (ED)	Class	ED measures the density of edges in a given landscape
Shape metrics		
Fractal dimension index (FRAC)	Class	FRAC reflects the shape complexity of patches from a given class (approaches 1 for shapes with very simple perimeters such as squares, and approaches 2 for more complex shapes)
Contiguity index (CONTIG)	Class	CONTIG assesses the spatial connectedness, or contiguity, of cells within a grid-cell patch, which provides an index on patch boundary configuration and thus patches shape (grows to 1 as patch contiguity, or connectedness, increases)
Aggregation metrics		
Patch density (PD)	Class	PD provides a simple measure of the extent of subdivision or fragmentation of the patch type
Percentage of like adjacencies (PLADJ)	Class	PLADJ measures the degree of aggregation of patch types and increases with the aggregation
Structural and LULC-based indicators		
Structural indicators		
Degree of soil sealing	Block and LOR	The Degree of soil sealing represents the percentage of impervious surfaces; i.e. surface that can neither evaporate water nor permit rainwater to penetrate (LI et al., 2011) and ranges from 0 to 100
Normalized difference vegetation index (NDVI)	Block and LOR	The NDVI represents the amount of healthy vegetation present into the considered landscape and ranges from −1 to +1; NDVI = $(\rho_{nir} - \rho_{red})/(\rho_{nir} + \rho_{red})$ where ρ_{nir} and ρ_{red} are the reflectance values in the near-infrared and red bands
Distance to city center (Dist_CC)	Block and LOR	Dist_CC represents the distance (km) from the central point the inner-city, located here on the Alexanderplatz, with the TV-tower
Floor Area Ratio (FAR)	Block and LOR	FAR represents the total area of built floors divided by the area of the considered parcel (Giridharan, Lau, & Ganesan, 2005)
LULC-based indicators		
Density of transport infrastructure (Dens_Transport)	LOR	Dens_Transport represents the relative extent of streets at LOR-level Dens_Transport = Area (streets)/Area (LOR)
Relative Extent of continuous urban fabric (Ext_Cont)	LOR	Ext_Cont represents the relative extent of the continuous urban fabric (Floor Area Ratio > 0.8) at LOR-level; Ext_Cont = Area (continuous)/Area (LOR)
Relative Extent of detached housing (Ext_Det)	LOR	Ext_Det represents the relative extent of detached housing (LULC = Residential and Floor Area Ratio < 0.8) at LOR-level; Ext_Det = Area (detached_housing)/Area (LOR)
Relative extent of green spaces (Ext_GS)	LOR	Ext_GS represents the relative extent of Green spaces (i.e. Forested and not Forested Green spaces) at LOR-level; Ext_GS = Area (Green Spaces)/Area (LOR)
Relative extent of water bodies (Ext_Water)	LOR	Ext_Water represents the relative extent of Water Bodies at LOR-level; Ext_Water = Area (Water Bodies)/Area (LOR)

transferred to vector-based maps at the block-level. In total eight commonly used landscape metrics were applied (Table 2; cf. Table A2 in Appendix for calculation methods).

Beyond the relationship between LST and the actual LU types, relationships between the spatial distribution of LST and the physical characteristics of the urban structure can be expected

(Li et al., 2011). To better define the structural drivers of LSTs independently from LU types, we focused on simple parameters available at the block-level (cf. Table 2). Apart from the integrated degree of soil sealing (DSS), (e.g. Thinh et al., 2002) and the normalized difference vegetation index (NDVI), (e.g. Kottmeier et al., 2007), we additionally considered the distance to the city center (Dist_CC) as well as the floor area ratio (FAR). Particularly, the building density (FAR), the degree of soil sealing and the NDVI are expected to influence LST significantly. To define urban patterns we studied the influence of aggregated indicators at an intermediate level. Therefore, we integrated five simple indicators, determining the relative extent of (1) transport infrastructures (Dens_Transport), (2) continuous urban fabric (Ext_Cont), (3) detached housing (Ext_Det), (4) green spaces (Ext_GS) and (5) water bodies (Ext_Water) with corresponding effects on LST in line with expectations (Bolund & Hunhammar, 1999; Gill et al., 2007; Schwarz et al., 2012). The data sources can be found in Table 1.

2.2.3. Statistical analyses of land-use patterns and LST

We performed a variance analysis to test how the LST's distribution is connected to varying LU types classes using the Kruskal–Wallis one-way analysis of variance by ranks (parametric statistical Shapiro–Wilk tests could not be applied). A pairwise Wilcoxon Rank Sum Test was carried out as post hoc test to enable a finer understanding of the relationships among the LU types (Hervé, 2012).

To study potential park cool islands (PCI) we compared LSTs in large urban green spaces in Berlin with measured LSTs in buffers located at 50, 100, 150, 200, and 250 m around each urban greenspace larger than 10 ha (accordingly with findings from Eliasson & Upmanis, 2000; Gill et al., 2007; Mathey et al., 2010). To test significant differences between LST and green spaces and their surroundings we again used Kruskal–Wallis one-way analysis of variance.

Pearson's correlation coefficients between values of LST and the several landscape metrics were calculated for each single block to highlight the influence of LU patterns on LST distribution. The significance of each correlation coefficient was determined using a two-tailed t-test (Augspurger, 2009; Li et al., 2011).

The zonal analysis method (Yuan & Bauer, 2007) was used to estimate LST at each 0.01 increment of the NDVI (from −1 to 1), at each 1% increment of the degree of sealing (from 0% to 100%), at each 0.01 increment of FAR (from 0 to 5) and at each 100 m increment of Dist_CC from (0 to 25 km). At each increment per indicator a mean LST value was obtained from all corresponding blocks.

Simple linear regression analyses were then performed to determine the explanatory power of land-use patterns indicators on LST (e.g. Li et al., 2011). Multiple linear regression analyses were finally performed to determine the relative and combined effects of the above mentioned aggregated parameters (independent variables) on the LST's distribution at 10 am and 10 pm. The choice of the most suitable model for each analysis was based on the Akaike's information criterion (AIC), a popular entropy-based evaluation criterion (Bozdogan, 1987).

2.3. Potential heat-stress-related risk

2.3.1. Indicators for the potential heat-related vulnerability and hazard

Following the introduced concept of heat stress risk, it is composed of hazard and vulnerability. According to Kovats and Hajat (2008) the hazard arises from hot atmospheric conditions. For a more accurate representation of the hazard in terms of human effectiveness, we used simulated air temperature distribution (instead of LST) assuming that (near-ground) air temperature is a more precise indicator as it includes the effects of LST and wind current with similar spatial variations (Eliasson & Svensson, 2003; Spronken-Smith & Oke, 1998). Thus, we used the modeled near-ground air temperature during *autochthonous weather* conditions in summer, available from the Environmental Atlas of the city of Berlin (BSDUDE, 2001–2013; cf. Table 1).

As introduced before, vulnerability is composed of sensitivity and exposure. Two age-specific sensitivity groups are taken here into account; elderly people (age equal to or greater than 65 years) and young children (younger than 6 years). The population density is used to estimate the exposure (Depietri et al., 2013; Scherer et al., 2013).

Several authors claim that the vulnerability of city dwellers toward intense heat load is more significant at night, since daytime vulnerability may be reduced by adaptive human activities and location choice, while the options to optimize sleeping conditions are rather limited (Gabriel & Endlicher, 2011; Kovats & Hajat, 2008; Lubner & McGeehin, 2008). We thus focused on nighttime (early morning) conditions and applied in accordance with available dataset the near-ground air temperatures at 6 am.

All of this information was spatially joined at the block level defined by the reference system of all spatial information offered by the Environmental Atlas of Berlin. The data sources can be found in Table 1.

2.3.2. Estimation of potential heat-stress risk

Extreme heat events causing heat waves are generally characterized by temperatures exceeding a certain threshold for several days, and especially by consecutive nights with high minimum temperatures (Lubner & McGeehin, 2008). Gabriel and Endlicher (2011), for example, considered temperatures exceeding the 95th-percentile of daily distribution as a threshold to qualify a period of heat stress. Moreover, several recent studies show that LU types and patterns directly (e.g. through increased local temperatures) and indirectly (e.g. through air pollution) affect the thermal comfort and health of the city dwellers (Harlan et al., 2006; Schwarz et al., 2012). Eliasson and Svensson (2003) have shown the direct influence of LU patterns on temperature distribution at different weather conditions during both day and night. We therefore assumed that heat waves affect absolute temperatures, while spatial temperature patterns stay mostly consistent (despite possible local modification due to changing weather conditions with potential cumulative effects in heat-loads). Accordingly, we defined the potential hazard to arise from the LU patterns which affect air temperature distribution in a way that the extreme temperatures are likely to be found in the same areas repetitively. The spatial distribution of the potential hazard is thus considered to be constant over time.

As risk assessments are generally based on the magnitude of hazardous events (i.e. heat events) to determine the risk (e.g. to die from heat stress) for vulnerable elements (e.g. elderly people), (IPCC, 2012) we defined here the potential risk r of vulnerable city dwellers v which are located across residential building blocks with potential climatic hazards h (cf. Eq. (1)). By applying statistical thresholds for the level of vulnerability (i.e. amount of elderly people and infants and the population density) and the level of spatial hazard (i.e. air temperature on the block-level) into four categories (levels) ranging from 0 (no vulnerability or hazard) to 3 (maximum vulnerability or hazard), we determined areas at potential risk (Table 3):

$$r_{block}^{1,2,3\ldots9} = v_{block}^{level} \times h_{block}^{level} \tag{1}$$

$$v_{block}^{level} = \left[\frac{P_{block}^{age}}{\sum P_{block}^{age} * 100}\right]_{block}^{level} \times \left[\frac{\sum P_{block}^{age}}{A_{block}}\right]_{block}^{level} \tag{2}$$

The highest hazard level is defined for air temperatures exceeding the 95th-percentile of the distribution (Gabriel & Endlicher, 2011). Then two other levels are defined respectively, the 90th-percentile

Table 3
Classification and calculation method for the indicators used for the estimation of the potential heat stress related risk.

Indicator/potential risk factor		Value	Signification	Calculation method	Comment
Potential demographical vulnerability	Population density per block	0	Relatively negligible density	Population density < 85th percentile ⟺ 129 inh./ha	The average density in Berlin is 57 inh./ha
		1	Relatively low density	Population density > 85th percentile ⟺ 129 inh./ha	
		2	Relatively medium density	Population density > 90th percentile ⟺ 211 inh./ha	
		3	Relatively high density	Population density > 95th percentile ⟺ 326 inh./ha	
	Vulnerable inhabitants per block	[0–1]	Percentage of vulnerable inhabitants (*i.e. younger than 6 and/or older than 65)* at block- level divided by 100	The Concentration of vulnerable inhabitants is multiplied by the inhabitants density to give more importance to the absolute amount of vulnerable inhabitants	The average amount of vulnerable inhabitants per block in Berlin is 20%
	Concentration of vulnerable inhabitants in a block	0	Not problematic concentration	Weighted concentration < 0.3 ⟺ max. concentration of vul. ihn. of 30% if Pop. dens. = 1	The weighted concentration ranges from 0 to 3 with a mean value of 0.08 and a standard deviation of 0.20
		1	Quite problematic concentration	Weighted concentration > 0.3 ⟺ max. concentration of vul. ihn. of 30% if Pop. dens. = 1	
		2	Problematic concentration	Weighted concentration > 0.6 ⟺ max. concentration of vul. ihn. of 60% if Pop. dens. = 1	
		3	Highly problematic concentration	Weighted concentration > 0.9 ⟺ max. concentration of vul. ihn. of 90% if Pop. dens. = 1	
Potential climatic hazard	Distribution of air temperatures	0	Negligible potential hazard	Air temperature < 85th percentile ⟺ Temp(06 am) = 16.54 °C	The mean modeled air temperature in the summer in Berlin is of 14.41 °C with a standard deviation of 2.42 °C
		1	Low potential hazard	Air temperature > 85th percentile ⟺ Temp(06 am) = 16.54 °C	
		2	medium potential hazard	Air temperature > 90th percentile ⟺ Temp(06 am) = 16.74 °C	
		3	high potential hazard	Air temperature > 95th percentile ⟺ Temp(06 am) = 16.92 °C	

and the 85th-percentile. For assessing vulnerability, we combined the share of vulnerable inhabitants per block (i.e. age younger than 6 or equal to or greater than 65 years) with the population density to avoid focusing on places with noticeable shares of vulnerable dwellers but small amount of them in absolute numbers (cf. Eq. (2)). In accordance with the potential climatic hazard estimation, we used the same classification method for population density to estimate the level of vulnerability (ranging from 0 to 3, cf. Eq. (2)). For the share of vulnerable inhabitants per block this approach was not convenient which is why we used thresholds (i.e. 0.3, 0.6 and 0.9) related to the density levels. A share of vulnerable inhabitants of 0.3 means that there are up to 10% of vulnerable inhabitant per blocks with a population density level of 3; 20% for level 2; and 30% for level 1 (Table 3).

According to this approach it can be expected that especially central located built-up areas provide high degrees of risk due to their physical conditions and the increasing population density towards the city center.

3. Results and discussion

3.1. Land-use patterns and surface temperature

3.1.1. Spatial pattern of SHUI

Fig. 3 indicates SUHI for Berlin. It reveals a trend of increasing LSTs towards the city center, especially at 10 pm. Local maxima occurred on bare soils of agricultural land at 10am and on water bodies at 10 pm due to their high thermic inertia (Fig. 2).

To describe surface urban heat islands (SUHIs) in Berlin we considered the magnitude [max LST – mean LST] (Schwarz et al., 2012), which on average is 8.7 °C at 10 am and 3.2 °C at 10 pm and the range, i.e. [max LST – min LST] which is 16.0 °C at 10 am and 19.7 °C at 10 pm. These results are related to the larger variability of LST at 10 am and the higher amount of extreme values at 10 pm. According to Kottmeier et al. (2007), SUHI in Berlin is less pronounced than in other large cities due to the relatively dry countryside, with prevailing agricultural land use on sandy soils. Another possibility of presenting the magnitude of SUHI is given in the Appendix, Fig. A8.

Fig. 4 displays the SUHIs in Berlin showing that SUHIs at 10 am are spread out around the city, especially on bare soils, non-forested green-spaces, industrial and commercial areas as well as on the airports; SUHIs at 10 pm are much more concentrated in the inner-city with its dense urban fabric.

In total, 15% (at 10 am) to 20% (at 10 pm) of city area are affected by SUHI, mainly qualified as 'Low SUHI' whereas the class 'High SUHI' only achieves 0.1% at both points in time. This extent is similar to other studies (e.g. Schwarz et al., 2012).

At 10 am 'Industrial and commercial uses' are associated with almost one third of the total SUHI, while they represent less than 10% at 10 pm. This could be explained by large amount of non-built-up sealed areas (i.e. large parking lots) with high daily insolation rates and high rates of nightly air ventilation causing rapid temperature increase at day and fast cooling at night. Direct heat release from industry may also play a role here (Li et al., 2011). At 10 pm around one third of the SUHI area can be found in 'Transport infrastructures' while it only represents 18% at 10am, indicating the relevance of this class towards nightly heat load. The contributions of 'Public and private facilities' and 'Mixed uses' to SUHI are constant with about 20% between 10 am and 10 pm. Interestingly, urban green spaces also contribute to SUHI's extent with around 15%, mainly assigned to 'Unforested green spaces'

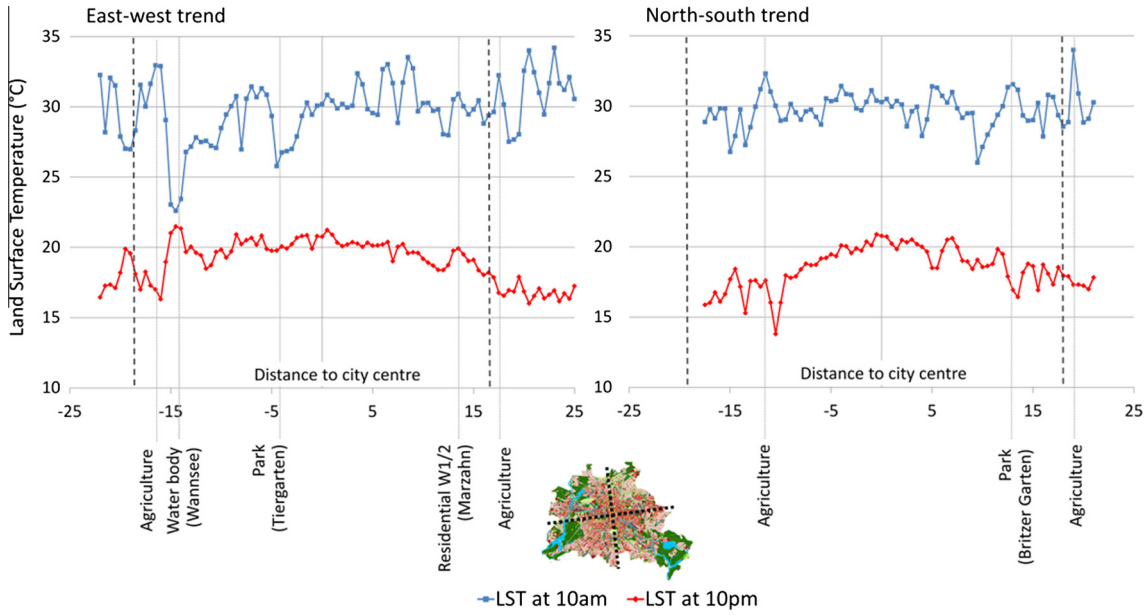

Fig. 3. East–West (left) and North–South (right) transversal distributions of LST in Berlin at 10 am (blue line) and 10 pm (red line) within the administrative border of Berlin (dark dotted lines). (For interpretation of the references to colour in this figure legend, the reader is referred to the web version of this article.)

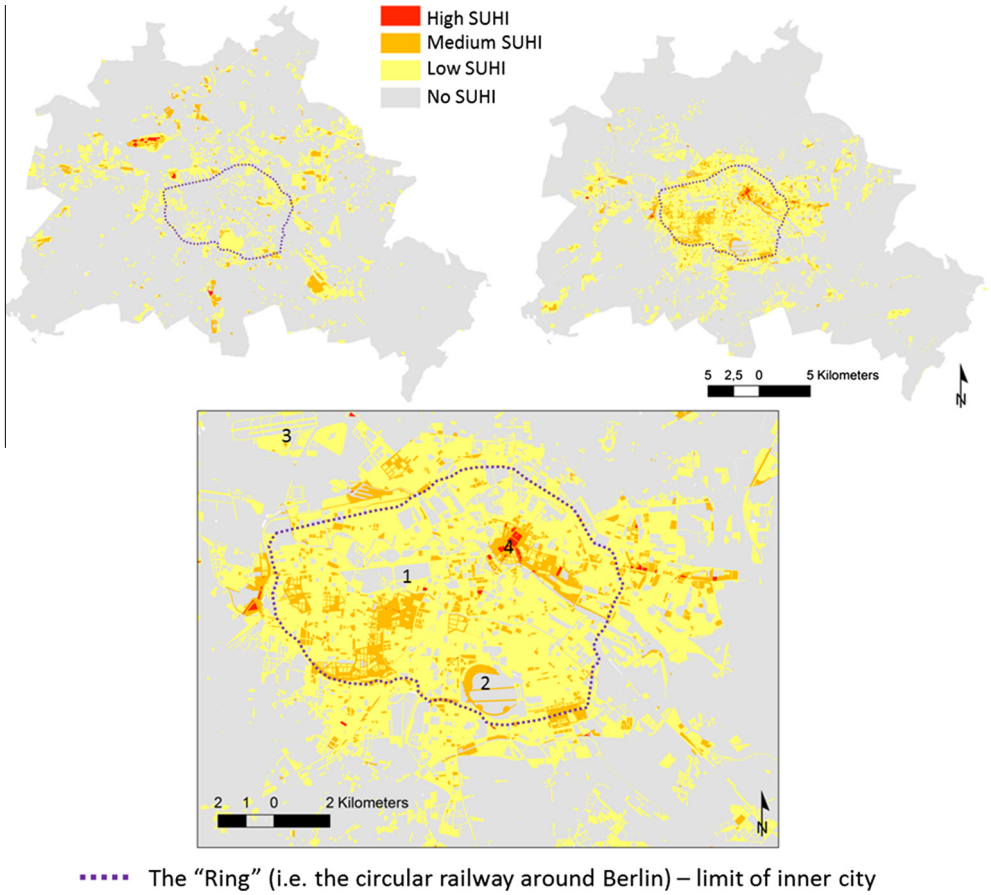

Fig. 4. Characterization of SUHI in mid-August 2000 at 10 am (above left) and at 10 pm (above right) with a focus on SUHI of the inner-city at 10 pm (below). We used the SUHI indicator developed by Zhang and Wang (2008): Area [*SUHI*] = Area [*LST* > (*mean LST* + 1 *standard deviation*)]. SUHI values are split into 3 categories (high, medium and low) of equal parts, ranging between (*meanLST* + *standard deviation*) and (*max LST*). For clearer results the uses 'Water bodies' have been excluded for 10 pm and 'Agricultural' for 10 am (Schwarz et al., 2012). Special sites: 1: The central park Tiergarten, 2: The urban park on the former Tempelhof airport, 3: Tegel airport, 4: TV Tower on the Alexander Platz.

(at 10 am) and 'Forested green spaces' (at 10 pm). As expected, the dense residential classes 'W1' and 'W2' contribute more to the SUHI extent at 10 pm with 21% than at 10 am with only 10% which strengthens the focus on nighttime temperature when studying the vulnerability of city dwellers towards heat stress. Less dense residential classes (W3 and W4) contribute negligibly to SUHI. The distribution across all LU types is shown in the Appendix, Fig. A1.

3.1.2. Land-use types and LST

The detailed results in Fig. 5 are fully consistent with findings about the SUHI extent (cf. Figs. 1 and 4). The warmest land uses both at 10 am and 10 pm are those that are highly sealed and/or densely built-up, such as 'Industrial and commercial uses', 'Mixed-uses', 'Public or private facility', 'Transport infrastructures', and most dense residential classes 'W1' and 'W2'. Non-built-up open land uses (i.e. 'Agricultural' uses', 'Unforested green spaces' or 'Urban brownfields') also exhibit large mean LSTs at 10 am as well as large variability in LST since they exhibit among the lowest LSTs at 10 pm. This might be due to the absence of tree cover preventing cooling through evapotranspiration over the day and enabling fresh air generation over the night (Mathey et al., 2010). 'Water bodies' show the smallest variability between 10 am and 10 pm due to the fact that water has the largest specific heat capacity associated with a slow cooling rate (Li et al., 2011).

According to Kottmeier et al. (2007), the standard deviation (SD) characterizes the variability arising from different physical surface properties or shading effects. This is also one reason for high SD values in 'Unforested green spaces' (2.04 °C at 10 am and 1.26 °C at 10 pm) and 'Forested green spaces' (1.81 °C at 10 am and 1.03 °C at 10 pm). The residential classes have relatively small SD values which are due to their structural homogeneity and the clear trend of a spatial distribution pattern from the city-center to the edge of the city (cf. Fig. 1).With the variance analysis, we tested for significant differences of LST in applied LU types. The results show that, with few exceptions, LSTs in all LU types are significantly different from one another at both points in time, stating that the selected LU types are suitable to study the importance of land uses as a driver for LST in Berlin (Appendix, Table A4). Non-significant differences of LST across LU types are explained by their different extents (cf. Fig. 1), the heterogeneity among the LU types (Appendix, Table A1), the similarities among certain types (e.g. 'Mixed-uses' and 'Residential W1', 'Public and private facilities' and 'Residential W2' or 'Agricultural' land and 'Urban brownfields').

The buffer-based park analysis showed that green spaces larger than 10 ha exhibit significantly different LSTs than their surroundings. 'Forested green spaces' are cooler, on average 1.2 °C for the distance of 50 m and 1.9 °C for the distance of 250 m (at 10 am) whereas non-forested ones and agricultural land show inversed results (i.e. LST significantly lower than their surroundings only at 10 pm), (Appendix, Fig. A2 and Table A5). These results indicate the park cooling-island-effect in Berlin and are consistent with the findings of several authors quoted in the review of Mathey et al. (2010). In line with this, we detected varying LSTs in different buffers around large parks showing the declining capability to decrease surrounding LSTs with increasing distance to the park (i.e. at 10 am, LST at a distance of 50 m tended to be significantly lower than LST at a distance of 250 m). However, (Spronken-Smith & Oke, 1998, 1999) as well as Eliasson and Upmanis (2000) have shown that the cooling influence of parks on their surroundings, the so-called park-breeze, should be estimated by air temperatures analysis on the small scale, which finds expression in their definition of air temperature, "representing the integrated effects of underlying surface microclimates after dilution by near-surface turbulent mixing and advection by the wind" (Spronken-

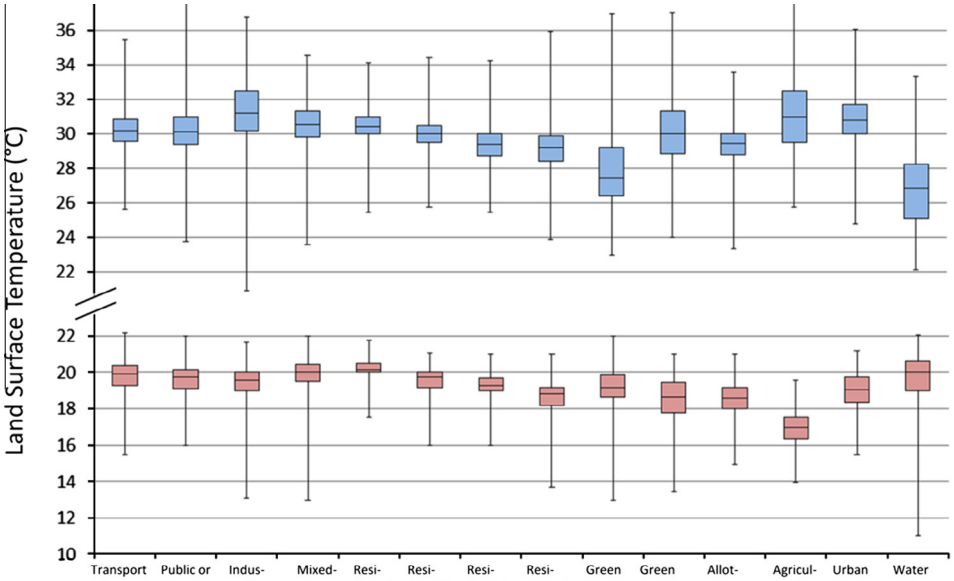

	Transport Infra-structure	Public or Private Facility	Indus-trial or Commer-cial uses	Mixed-uses	Resi-dential _W1	Resi-dential _W2	Resi-dential _W3	Resi-dential _W4	Green Spaces Fores-ted	Green Spaces Not-Forested	Allot-ment Garden	Agricul-tural	Urban Brown-field	Water Body
Mean LST (°C)	30.2	30.1	31.4	30.5	30.5	30.0	29.4	29.1	27.9	30.1	29.3	31.2	30.8	26.7
	19.7	19.6	19.4	19.9	20.2	19.6	19.3	18.8	19.5	18.5	18.6	16.9	19.0	19.8
Standard Deviation	1.14	1.45	1.64	1.29	0.84	0.87	0.99	1.06	1.81	2.04	1.24	2.09	1.56	1.56
	0.86	0.83	0.92	0.85	0.51	0.67	0.57	0.69	1.03	1.26	0.84	0.97	0.97	0.97
Δ Total mean LST	+	+	+++	++	++	+	-	--	---	+	--	+++	+++	----
	++	+	+	++	++	+	/	-	/	--	--	---	/	++

Fig. 5. Boxplots, mean values, and the standard deviation of LST among each land-use type at 10 am (above) and 10 pm (below); Δ Total mean LST exhibits the difference of the mean LST per LU type compared to the total mean LST of the study area (/ no significant difference, +/− positive or negative difference of at least 0.2 °C, ++/−− difference of at least 0.5 °C, +++/−−− difference of at least 1 °C).

Smith & Oke, 1998). Despite the lack of information on near-surface phenomena, the significant differences in LSTs in successive buffer rings indicate the capability of large forested parks to decrease surrounding LSTs, especially in the daytime (cf. Appendix, Table A5).

3.1.3. Landscape metrics and LST

At the landscape-level, Simpson's evenness and diversity indexes (SIEI and SIDI) correlate stronger with LST at 10 am than at 10 pm with moderate and almost equal values of 0.32 for SIDI and 0.33 for SIEI. It is thus hard to conclude whether LST's distribution among LU types is more influenced by their evenness or their diversity.

At the class-level (Table 4) the highest correlations of LST and landscape metrics were ascertained for 'Forested green spaces', 'Transport infrastructures' and 'Water bodies', and to a lesser extent for 'Agricultural' lands and 'Industrial and commercial' uses (Table 4). In general, correlation coefficients are relatively low due to high spatial variability in the classes. Still, conclusions can be made on how the spatial LU patterns affect LST by comparing the class results for the two points in time.

For 'Forested green spaces', all correlations are negative proving the cooling effects of this class. The higher correlations of LST for 10 am with PLAND, FRAC and CONTIG show that large patches with complex shapes (e.g. star-shaped or palmate) reduce LST significantly. Negative correlations of LST (at 10 am) with PD and PLADJ show that interconnected and spatially aggregated 'Forested green spaces' have positive effects on LST in the morning. Correlations for 10 pm are less strong and often not even significant. These findings are not fully consistent with the study of Li et al. (2011) who conclude for Shanghai (China) that urban green areas reduce SUHI more effectively when scattered across the urban landscape than when concentrated. These opposite conclusions emerge from different LU patterns and climatic conditions in both cities and show that results can vary considerably depending on the regional conditions and the data applied.

For 'Transport infrastructures' all correlations are positive, showing the warming effect in this class. The stronger correlations of LST with PLADJ and FRAC indicate that LST increases at 10 am with increasing shape complexity and interconnectedness of corresponding patches. For 10 pm, the stronger correlations with PLAND and CONTIG indicate that the extent of this use and the adjacency of corresponding LU patches are an important driver of LST increase at 10 pm.

The structural characteristic of 'Industrial and commercial' uses affect LST distribution predominantly at 10 am. PLAND, FRAC, CONTIG and PLADJ show that an increase of size, complexity and aggregation of corresponding patches leads to an increase in LST. Residential uses (all residential classes) do not allow a clear conclusion due to the large variety of patch structures. Determining the influence of residential uses on LST was achieved using aggregated indicators at the LOR-level (see results below).

Concluding, the analysis at the class-level reveals the influence of spatial patterns for selected LU types but is not suitable for deriving general conclusions on quantitative effects on SUHI for different urban pattern configurations. One reason for that is the complexity of landscape metrics itself, especially when applied to large highly diverse urban landscapes and the consideration within independently considered LU types (Harbin & Jianguo, 2004). Weng et al. (2007) and Schwarz (2010) argue that landscape metrics might give better results when comparing relationships of LU patterns and LSTs for different urban areas (or different parts within one urban area) as we do in the following.

3.1.4. Structural and LU-based indicators and LST (Block and LOR-level)

Fig. A7 in the appendix displays the applied structural indicators as a function of LST at both points in time and shows respective linear regression results at the block level. We obtained the degree of soil sealing to be the best predictor of LST-variations at 10 am and 10 pm. However, under certain conditions other parameters were better predictors, such as NDVI when excluding extreme values or the distance to the city center within a 20 km radius from the center, and also FAR at 10 pm when values larger than 3 were excluded (Appendix, Fig. A7).

According to Li et al. (2011), the relationships between LST and structural parameters are scale dependent and correlations are usually higher at coarser scale. However, Table 5 shows that structural indicators at the LOR-level exhibit similar but less strong correlations with LST (except for FAR and NDVI) than obtained on the block-level (Appendix, Fig. A7). This can be explained by the use of the zonal statistic method, which enabled to significantly increase the correlation values on the block-level (cf. Yuan & Bauer, 2007).

Table 4
Pearson correlation coefficients between LST and class-level metrics at 10 am (gray lines) and 10 pm (white lines); bold values (with $|r| \geq 0.3$) indicate a linear dependence.

	Transport Infra-structure	Public and Private Facility	Industrial and Commercial	Mixed use	All Residential uses	Forested green space	Not-forested green space	Allotment garden	Agricultural	Urban brownfield	Water Body
Area and Edge Metrics											
PLAND	**.38** **	.14 **	**.31** **	.19 **	.09 *	**-.55** **	.10 *	-.01	.13 **	.11 *	**-.43** **
	.39 **	.15 **	.07	.22 **	-.01	-.15 **	-.23 **	-.19 **	**-.36** **	-.04	.14 **
ED	**.34** **	.15 **	.28 **	.20 **	.10 *	-.26 **	.09 *	-.01	.08 *	.11 *	**-.33** **
	.18 **	.20 **	.09 *	.25 **	.01	-.02	-.18 **	-.17 **	**-.34** **	-.04	.08
Shape Metrics											
FRAC	**.42** **	.18 **	**.30** **	.23 **	.20 *	**-.40** **	.09 *	.01	.10 *	.12 **	**-.37** **
	.19 **	.25 **	.11 *	**.31** **	.11 *	-.07	-.20 **	-.17 **	**-.40** **	-.04	.09
CONTIG	**.41** **	.17 **	**.31** **	.22 **	.18 **	**-.48** **	.09 *	.01	.11 *	.11 *	**-.40** **
	.30 **	.22 **	.10 *	.29 **	.10 *	-.13 **	-.21 **	-.17 **	**-.40** **	-.04	.11 *
Aggregation Metrics											
PD	**.35** **	.16 **	.30 **	.22 **	.12 *	**-.31** **	.10 *	.01	.10 *	.12 **	**-.34** **
	.12 **	.25 **	.12 **	.29 **	.04	-.02	-.19 **	-.18 **	**-.39** **	-.04	.08
PLADJ	**.44** **	.17 **	**.31** **	.23 **	.19 **	**-.47** **	.09 *	.01	.11 *	.12 **	**-.40** **
	.29 **	.24 **	.10 *	**.30** **	.10 *	-.12 **	-.21 **	-.18 **	**-.40** **	-.04	.10 *

Significance levels of the p-values: '**' = 0.01; '*' = 0.05

Table 5
Pearson's correlation coefficients between aggregated indicators and mean LSTs for 10 am and 10 pm at LOR-level.

	Structural indicators				*LULC-based indicators*				
	DSS	NDVI	Dist_CC	FAR	Dens_Transport	Ext_Cont	Ext_Det	Ext_GS	Ext_Water
Mean LST 10 am	.52**	−.53**	−.33**	.33**	.18**	.43**	−.28**	−.37**	−.40**
Mean LST 10 pm	.71**	−.63**	−.54**	.60**	.41**	.59**	−.40**	−.35**	−.05

* $p = 0.05$.
** $p = 0.01$.

At the LOR-level, the variation of LST is better explained by structural indicators at 10 pm, confirmed by higher correlation coefficients, matching the insights of the block-level analysis (Appendix, Fig. A7). LU-based indicators exhibit only moderate correlations with LST and are thus less convenient in uncovering the effect of the urban patterns on temperature distribution. All indicators except for 'Ext_GS' and 'Ext_Water' are more suitable to explain LST variation at 10 pm showing that LST is likely to be stronger linked to the extent of built-up areas at that time.

Using the zonal statistic method (Yuan & Bauer, 2007) did not enable to carry out multiple linear regressions at the block-level; we thus carried them out at the coarser LOR-level. To provide a maximum return on the explanation of LST from structural and LU-based indicators, we first carried out separate multiple regression analyses for both types of indicators before integrating them in a combined manner (Appendix, Table A7). The best multiple regression model contained all aggregated structural and LU-based indicators and explained 56% percent of LST variation at 10 pm (51% at 10 am), which is less than the degree of soil sealing alone using the zonal statistic method at the block-level.

These results show that a considerable proportion of LST variation cannot be explained by the applied indicators. Kolokotroni and Giridharan (2008), e.g., found that surface albedo is the most critical driver of outdoor temperatures in London (UK). Spronken-Smith and Oke (1998) revealed that the presence or absence of shade, the surface albedo, and the state of water availability are the main drivers for LST variation (on unsealed areas). Yuan and Bauer (2007) proved the relevance of soil water content and Gill et al. (2007) found that the climatic benefits of green spaces can be largely reduced in case of drought, indicating a declining cooling capacity of green spaces in the course of a heat event. On the other hand, Spronken-Smith and Oke (1998) showed for Vancouver that the relative cooling of parks develops rapidly at low cloud cover after sunset, especially in areas of dry and open surfaces.

Moreover, the relationship between urban structure and LST pattern is strongly affected by the time of observation. Eliasson and Svensson (2003) showed that stepwise multiple regression analyses determining the relative effects of land use and other parameters on air temperature patterns exhibit different results under different seasons, different points of time over the day, and different weather conditions (i.e. clear and calm or cloudy and windy). Multi-temporal LST data-sets would allow to study dynamics in the course of a heat event and under different local weather conditions taking into account the relevant factors cloudiness, humidity and wind speed (Eliasson & Svensson, 2003; Kolokotroni & Giridharan, 2008).

3.2. Potential heat-stress risk for city dwellers

Fig. 6 displays the potential risk in Berlin integrating the heat stress hazard (using simulated air temperatures for 6 am at block-level) and the vulnerability (population density and the share of vulnerable people at the block-level). The potential risk is divided into six categories ranging from extremely high to negligible risk. With some exceptions the majority of blocks potentially at risk are situated in central residential areas of Berlin inside the "Ring" (Fig. 6). Outside the "Ring" potential risk occurs in the neighborhood of Friedenau and in the western part of the district Lichtenberg which partly achieves the highest risk potential despite the considerable distance to the city center, which is attributed to the high amount of elderly residents. Inside the "Ring" an accumulation of the risk is seen in western parts comprising highly dense residential uses ('Residential W1') with a comparably high amount of elderly residents. The residential area to the east of the former airport Tempelhof, commonly considered to be problematic in terms of heat load because of the dense built-up areas, exhibits a moderate potential risk as a consequence of the population structure. Blocks with extremely high risk occur only in very low numbers in the densest areas of Berlin in the south-west of Alexanderplatz. When focusing on potential risks from extremely high to medium, two major residential areas can be identified: firstly, areas composed of mid-rise dense urban fabric (i.e. inner-city blocks mainly from Wilhelminian time) covering the largest part of residential uses inside the "Ring"; and secondly, areas mostly composed of high-rise prefabricated multi-story houses (built after the Second World War mainly in the eastern part of Berlin).

Table 6 shows the number of concerned blocks per risk class as well as the specific extent as percentage of the residential area at risk. The Table also gives the number of blocks derived from the potential risk combination indicating whether the risk results more from vulnerability or hazard. For example, 19 blocks have a 'high potential risk' (class 6) from the combination of a high potential vulnerability (class 3) with a medium potential climatic hazard (class 2) and 128 from the opposite combination (vulnerability = class 2 and hazard = class 3). In case of two possible combinations per risk class, more blocks derive from the combination with higher potential climatic hazard which results from the defined thresholds per indicator. The mean population density in Berlin is, with 60 capita/ha, relatively low compared to other major cities, such as Paris (France) with a population density of around 210 capita/ha. In this context, chosen thresholds (fixed to 129 capita/ha, 211 capita/ha and 326 capita/ha) can be considered to be suitable and representative.

Despite their importance in the literature (Depietri et al., 2013; Fouillet, Rey, Wagner, Laaidi, et al., 2008), we did not consider poverty and social isolation as indicators to define the vulnerability of the city dwellers towards heat stress, and refer to Gabriel and Endlicher (2011), who showed that age is the most critical indicator in Berlin. However, in other cities socio-economic indicators might be crucial to characterize the local vulnerability. Rowland (2008) suggests that vulnerability toward heat-related illnesses among infants and young children is likely to be associated with dependency factors and pre-existing illness, which should be considered more specifically to better define heat-related child vulnerability.

To conclude, it could be shown to which extent varying LU patterns with specific temperature characteristics affect the potential heat-stress risk in the city. However, clear links between LU pattern-describing indicators (cf. Table 2) and the potential risk are

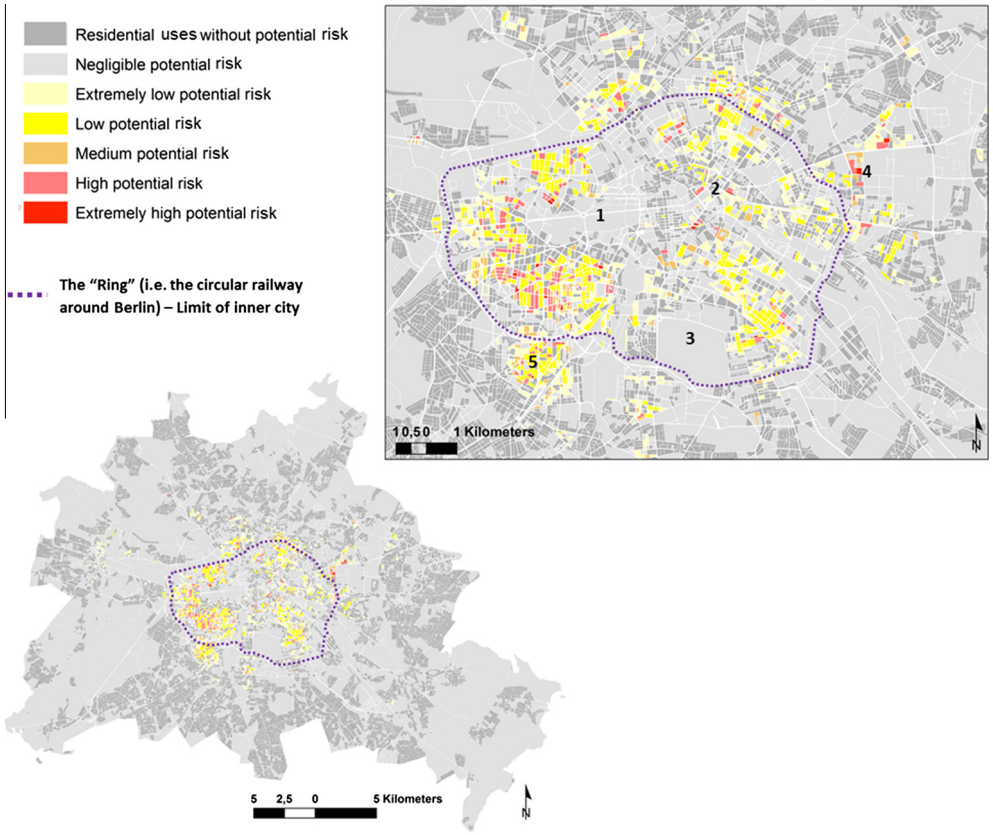

Fig. 6. Risk map, valuing the potential heat-stress risk per block; Special sites: 1: The central park Tiergarten, 2: TV Tower on the Alexander Platz, 3. The urban park on the former Tempelhof airport, 4. Western part of the district Lichtenberg, 5: Neighborhood of Friedenau.

Table 6
Description of potential risk (potential dwellers' v 490 ulnerability* potential climatic hazard), sum of concerned blocks and extent of potential risk areas as a percentage of the total residential area of Berlin.

Potential risk class		Potential dwellers' vulnerability	Potential climatic hazard	Number of concerned blocks	Percentage of Berlin's residential area
Extremely high potential risk	9	3	3	21	0.08
High potential risk	6	3	2	19	0.95
		2	3	128	
Medium potential risk	4	2	2	138	0.78
Low potential risk	3	3	1	33	3.53
		1	3	422	
Extremely low potential risk	2	2	1	126	4.70
		1	2	496	
Negligible potential risk	1	1	1	336	2.40

more difficult to derive (cf. Appendix, Fig. A5). The strongest linear relationship was obtained for FAR and the potential risk (adjusted $R^2 = 0.58$) indicating that the building density is most suitable to describe the hazard component of the heat-stress risk (independently from its location in the city, the natural characteristic of its surrounding, the state of the surfaces and the characteristics of the inhabitants). The link between heat-stress risk and LU patterns needs to be further studied under inclusion of objective heat-stress indicators derived from morbidity and mortality data (e.g. Scherer et al., 2013).

3.3. Implications for city planners

Adaptation and mitigation strategies are necessary for areas of higher risk especially in view of future climate change and the probable increment of heat events and the proceeding aging of the urban population (e.g. Lafortezza, Carrus, Sanesi, & Davies, 2009; Lauf et al., 2012b). Such strategies can, firstly, address vulnerability, for instance, by reducing the amount of vulnerable people (e.g. by promoting individual relocation for instance with economic stimuli) or by reducing the exposure of vulnerable people by installing air conditioning systems. Secondly, the local hazard can be addressed by changing the local environmental settings, e.g. by increasing the vegetation density by street trees, roof or facade greenery (Gill et al., 2007) or by directing urban development while taking into account the insights of this study (Section 3.1). Forested or partly forested green space infrastructures should be promoted allowing for local cooling, soil sealing should be decreased to increase latent heat radiation and built-up structures could be transformed in a way to enable aeration of dense built-up structures. The change of local building structure addresses both the reduction of vulnerability by reducing population density and

the reduction of hazardous heat load, but is by far the most complicated measure in terms of practicability. However, the variety of strategies shows that mitigation of and adaptation to heat stress can proceed on the individual and on the societal level, whereas the second depends mainly on decision-makers addressing urban planning. Fouillet et al. (2008) have for instance shown that several preventive measures aiming at reducing the risks related to high temperatures are likely to have played a major role in reducing heat-stress related mortality during the 2006 heat wave compared to 2003. In any case, the proceeding demographic and climatic change will increasingly challenge urban planners and city-dwellers in the future and requires intelligent adaptation and mitigation strategies (Patino & Duque, 2013).

4. Conclusions

In this study on Berlin we showed, firstly, how different parameters defining the LU pattern and structure influence the LST distribution for two different points in time of a typical summer day using statistical analysis. Secondly, we assessed the potential heat wave related heat-stress risk in a spatially explicit manner by identifying the vulnerable amount of city-dwellers and the local hazard based on the urban pattern and structure.

SUHI was significantly influenced both by the LU composition and the structure configuration of the urban fabric. We identified main drivers of LST as well as relevant urban patterns influencing LST. The degree of soil sealing was the best predictor of LST in summer time. Under certain conditions other indicators had stronger abilities to explain LST variations, such as NDVI under exclusion of extreme values, the distance to city center within a radius of 20 km and the floor area ratio at 10 pm. Moreover, we found that (even though dispersed vegetation is important to regulate urban temperatures) large and/or spatially aggregated green spaces are more important for the reduction of LST in Berlin. Conversely, clustered and interconnected transport areas tended to largely increase LST. The potential cooling effect of green spaces highly depended on the degree of tree cover. Forested green spaces reduced LST to greater amounts at 10 am while non-forested ones only decrease LST at 10 pm. The multiple regression model developed in this study (under its constraints) explained 56% percent of LST variation in Berlin. Additional parameters, such as albedo, characteristics of construction material or more detailed local weather conditions as well as multi-temporal approaches might further improve these results.

Relating to the analysis on how the LU patterns affect the urban temperatures patterns, we presented a simple method to analyze the potential heat-stress risk across the city by considering urban air temperatures and the concentration of vulnerable inhabitants at the small-scale block level. High potential risk was only found to a low extent, mainly but not solely in the dense urban fabric of the inner-city. These critical areas must be addressed by urban planners to mitigate heat-related death rates in cases of intense heat waves (Scherer et al., 2013). We argue that in those areas further soil sealing should be avoided and vegetation density should be increased. In reurbanizing cities such as Berlin, suitable sites for new built-up areas should be identified at an adequate distance from such risk prone areas to control building density. This indicates a potential conflict towards the concept of the compact city of short distances (reducing energy consumption and climate effective emission), followed by many German municipalities.

The proposed analyses allow identifying areas at risk of heat-stress which becomes crucial for resilient urban design. The presented results support sound decision-making to urban planner by identifying sensitive areas to increasing heat-stress-related risks The combination of LU modeling integrating the dynamics of demographic change and microclimate simulations would additionally beneficial for the early prevention of future risks (e.g. Grossman-Clarke, Stefanov, & Zehnder, 2011; Lauf, Haase, Seppelt, & Schwarz, 2012a; Lauf et al., 2012b; Meier & Scherer, 2012).

Acknowledgement

This article is a contribution of the UCaHS-project –*Urban Climate and Heat Stress in mid-latitude cities in view of climate change* funded by the German research foundation (DFG-Research Unit 1736). The authors thank the Berlin Senate Department for Urban Development and Environment for data provision. Further we want to thank Kyle Pipkins for polishing the language of the manuscript.

Appendix A. Supplementary material

Supplementary data associated with this article can be found, in the online version, at http://dx.doi.org/10.1016/j.compen vurbsys.2014.07.005.

References

Augspurger, C. (2009). *Table of critical values for Pearson's correlation coefficients*. <http://www.life.illinois.edu/ib/203/Fall%2009/PEARSONS%20CORRELATION%20COEFFICIENT%20TABLE.pdf> 06.06.13.

Birkmann, J., Cardona, O. D., Carreno, M. L., Barbat, A. H., Pelling, M., Schneiderbauer, S., et al. (2013). Framing vulnerability, risk and societal responses: The MOVE framework. *Natural Hazards, 67*, 193–211.

Bolund, P., & Hunhammar, S. (1999). Ecosystem services in urban areas. *Ecological Economics, 29*, 293–301.

Bozdogan, H. (1987). Model selection and Akaike's information criterion (AIC) – The general theory and its analytical extensions. *Psychometrika, 53*(3), 345–370.

BSDUDE (2001–2013). Berlin Senate Department for Urban Development and the Environment. *Urban and Environmental Information System (UEIS), 1992–2013: Environmental Digital Atlas*. <http://www.stadtentwicklung.berlin.de/umwelt/umweltatlas/edua_index.shtml> 15.05.13.

Cao, X., Onishi, A., Chen, J., & Imura, I. (2010). Quantifying the cool island intensity of urban parks using ASTER and IKONOS data. *Landscape and Urban Planning, 96*, 224–231.

Chang, C. R., Ming-Huang, L., & Shyh-Dean, C. (2007). A preliminary study on the local cool-island intensity of Taipei city parks. *Landscape and Urban Planning, 80*, 386–395.

Cutter, S. L. (1996). Vulnerability to environmental hazards. *Progress in Human Geography, 20*(4), 529–539.

Depietri, Y., Welle, T., & Renaud, F. G. (2013). Social vulnerability assessment of the Cologne urban area (Germany) to heat waves: Link to ecosystem services. *International Journal of Disaster Reduction, 6*, 98–117.

Eliasson, I., & Upmanis, H. (2000). Nocturnal airflow from urban parks – Implications for city ventilation. *Theoretical and Applied Climatology, 66*, 95–107.

Eliasson, I., & Svensson, M. K. (2003). Spatial air temperature variations and urban land use – A statistical approach. *Meteorological Application, 10*, 135–149.

Fouillet, A., Rey, G., Wagner, V., Laaidi, K., et al. (2008). Has the impact of heat waves on mortality changed in France since the European heat wave of summer 2003? A study of the 2006 heat wave. *International Journal of Epidemiology, 37*, 309–317. http://dx.doi.org/10.1093/ije/dym253.

Gabriel, K. M. A., & Endlicher, W. R. (2011). Urban and rural mortality rates during heat waves in Berlin and Brandenburg, Germany. *Environmental Pollution, 159*, 2044–2050.

Gallopin, G. C. (2006). Linkages between vulnerability, resilience, and adaptive capacity. *Global Environmental Change, 16*, 293–303.

Gill, S. E., Handley, J. F., Ennos, A. R., & Pauleit, S. (2007). Adapting cities for climate change – The role of the green infrastructure. *Built Environment, 33*(1), 115–133.

Giridharan, R., Lau, S. S. Y., & Ganesan, S. (2005). Nocturnal heat island effect in urban residential developments of Hong Kong. *Energy and Buildings, 37*, 964–971.

Gross, G. (1993). *Numerical simulation of canopy flows*. Berlin and Heidelberg: Springer.

Grossman-Clarke, S., Stefanov, W. L., & Zehnder, J. A. (2011). Urban weather, climate and air quality modeling: increasing resolution and accuracy using improved urban morphology. In X. Yang (Ed.), *Urban remote sensing: Monitoring, synthesis and modeling in the urban environment* (pp. 305–319). Chichester, UK: John Wiley & Sons, Ltd.

Harbin, L., & Jianguo, W. (2004). Use and misuse of landscape indices. *Landscape Ecology, 19*, 389–399.

Harlan, S. L., Brazel, A. J., Prashad, L., Stefanov, W. L., & Larsen, L. (2006). Neighborhood microclimates and vulnerability to heat stress. *Social Science & Medicine, 63*, 2847–2863.

Harlan, S. L., Declet-Barreto, J. H., Stefanov, W. L., & Petitti, D. B. (2013). Neighborhood effects on heat deaths: Social and environmental predictors of vulnerability in Maricopa County, Arizona. *Environmental Health Perspectives, 121*(2), 197–204.

Herold, M., Scepan, J., & Clarke, K. C. (2002). The use of remote sensing and landscape metrics to describe structures and changes in urban land uses. *Environment and Planning, 34*, 1443–1458.

Hervé, M. (2012). *RVAideMemoire – Diverse basic statistical and graphical functions. R package version 0.9-11*. <http://CRAN.R-project.org/package=RVAideMemoire> 10.11.12.

Johnson, D. P., Stanforth, A., Lulla, V., & Luber, G. (2012). Developing an applied extreme heat vulnerability index utilizing socioeconomic and environmental data. *Applied Geography, 35*(1–2), 23–31.

Kolokotroni, M., & Giridharan, R. (2008). Urban heat island intensity in London – An investigation of the impact of physical characteristics on changes in outdoor air temperature during summer. *Solar Energy, 82*, 986–998.

Kottmeier, C., Biegert, C., & Corsmeier, U. (2007). Effects of urban land use on surface temperature in Berlin: Case Study. *Urban Planning Development, 133*, 128–137.

Kovats, R. S., & Hajat, S. (2008). Heat stress and public health – A critical review. *Annual Review of Public Health, 29*, 41–55.

IPCC (2012). Managing the risks of extreme events and disasters to advance climate change adaptation. In: C. B. Field, T.F. Stocker, D. Qin, D.J. Dokken, K.L. Ebi, M.D. Mastrandrea, K.J. Mach, G.K. Plattner, S.K. Allen, M. Tignor & P.M. Midgley (Eds.), Special Report of Working Groups I and II of the Intergovernmental Panel on Climate Change. New York: Cambridge, UK.

Ishigami, A., Hajat, S., Kovats, R. S., Bisanti, L., Rognoni, M., Russo, A., et al. (2008). An ecological time-series study of heat-related mortality in three European cities. *Environmental Health, 7*(1), 5.

Lafortezza, R., Carrus, G., Sanesi, G., & Davies, C. (2009). Benefits and well-being perceived by people visiting greens paces in periods of heat stress. *Urban Forestry & Urban Greening, 8*, 97–108.

Lauf, S., Haase, D., Seppelt, R., & Schwarz, N. (2012a). Simulating demography and housing demand in an urban region under scenarios of growth and shrinkage. *Environment and Planning B, 39*(2), 229–246.

Lauf, S., Haase, D., Hostert, P., Lakes, T., & Kleinschmit, B. (2012b). Uncovering land-use dynamics driven by human decision-making – A combined model approach using cellular automata and system dynamics. *Environmental Modelling and Software, 27*(28), 71–82.

Lauf, S., Haase, D., & Kleinschmit, B. (2014). Linkages between ecosystem services provisioning, urban growth and shrinkage – A comparative modeling approach assessing ecosystem service trade-offs. *Ecological Indicator, 42*, 73–94.

Li, J., Song, C., Cao, L., Zhu, F., Meng, M., & Wu, J. (2011). Impacts of Landscape structures on surface heat islands – A case study of Shanghai, China. *Remote Sensing of Environment, 115*, 3249–3263.

Lubner, G., & McGeehin, M. (2008). Climate change and extreme heat events. *American Journal of Preventive Medecine, 35*(5), 429–435.

Mathey, J., Rößler, S., Lehmann, I., Bräuer, A., Goldberg, V., Kurbjuhn, C. et al. (2010). *Noch wärmer, noch trockener? Stadtnatur und Freiraumstrukturen im Klimawandel*. Naturschutz und Biologische Vielfalt, Heft 111. Bundesamt für Naturschutz. Bonn (Germany).

Mathey, J., & Rößler, S. (2011). Urban green space – Potentials and constraints for urban adaptation to climate change. *Proceedings of the global forum 2010. Resilient cities – Cities and adaptation to climate change, local sustainability* (Vol. 1, pp. 479–485).

McGarigal, K., Cushman, S. A., & Ene, E. (2012). *FRAGSTATS v4 – Spatial pattern analysis program for categorical and continuous maps*. Computer software program produced by the authors at the University of Massachusetts, Amherst. <http://www.umass.edu/landeco/research/fragstats/fragstats.html> 05.09.12.

Meier, F., & Scherer, D. (2012). Spatial and temporal variability of urban tree canopy temperature during summer 2010 in Berlin, Germany. *Theoretical and Applied Climatology, 110*, 373–384.

Oke, T. R. (1982). The energetic basis of the urban heat-island. *Quarterly Journal of the Royal Meteorological Society, 108*, 1–24.

Oudin Åström, D., Bertil, F., & Joacim, R. (2011). Heat wave impact on morbidity and mortality in the elderly population: A review of recent studies. *Maturitas, 69*(2), 99–105.

Patino, J. E., & Duque, J. C. (2013). A review of regional science applications of satellite remote sensing in urban settings. *Computers, Environment and Urban Systems, 37*, 1–17.

Reid, C. E., O'Neill, M. S., Gronlund, C. J., Birnes, S. J., Brown, S. J., Diez-Roux, A. V., et al. (2009). Mapping community determinants of heat vulnerability. *Environmental Health Perspectives, 11*(117), 1730–1736.

Romero-Lankao, P., Qin, H., & Dickinson, K. (2012). Urban vulnerability to temperature-related hazards: A meta-analysis and meta-knowledge approach. *Global Environmental Change, 22*, 670–683.

Rowland, T. (2008). Thermoregulation during exercise in the heat in children – Old concepts revisited. *Journal of Applied Physiology, 105*(2), 718–724.

Scherer, D., Fehrenbach, U., Lakes, T., Lauf, S., Meier, F., & Schuster, C. (2013). Quantification of heat-stress related mortality hazard, vulnerability and risk in Berlin, Germany. *Die Erde, 144*(3–4), 238–259.

Schneider, S. H., Semenov, S., Patwardhan, A., Burton, I., Magadza, C. H. D., Oppenheimer, M., et al. (2007). Assessing key vulnerabilities and the risk from climate change. Climate change 2007: Impacts, adaptation and vulnerability. *Contribution of working group II to the fourth assessment report of the intergovernmental panel on climate change*. Cambridge: Cambridge University Press.

Schwarz, N. (2010). Urban form revisited – Selecting indicators for characterizing European cities. *Landscape and Urban Planning, 90*, 29–47.

Schwarz, N., Schlink, U., Franck, U., & Grossmann, K. (2012). Relationships of land surface and air temperature and its implications for quantifying urban heat island indicators – An application for the city of Leipzig (Germany). *Ecological Indicators, 18*, 693–704.

SOBB (2013). Statistical Office Berlin Brandenburg. *Population data*. <https://www.statistik-berlin-brandenburg.de/datenbank/inhalt-datenbank.asp> 10.04.13.

Spronken-Smith, R. A., & Oke, T. R. (1998). The thermal regime of urban parks in two cities with different summer climates. *International Journal of Remote Sensing, 19*(11), 2085–2104.

Spronken-Smith, R. A., & Oke, T. R. (1999). Scale modelling of nocturnal cooling in urban parks. *Boundary-Layer Meteorology, 93*(2), 287–312.

Thinh, N. X., Arlt, G., Heber, B., Hennersdorf, J., & Lehmann, I. (2002). Evaluation of urban land-use structures with a view to sustainable development. *Environmental Impact Assessment Review, 22*, 475–492.

Weng, Q., Lub, D., & Schubringa, L. (2004). Estimation of land surface temperature-vegetation abundance relationship for urban heat island studies. *Remote Sensing of Environment, 89*, 467–483.

Weng, Q., Liu, H., & Lu, D. (2007). Assessing the effects of land use and land cover patterns on thermal conditions using landscape metrics in city of Indianapolis, United States. *Urban Ecosystems, 10*, 203–219.

Yuan, F., & Bauer, M. E. (2007). Comparison of impervious surface area and normalized difference vegetation index as indicators of surface urban heat island effects in Landsat imagery. *Remote Sensing of Environment, 106*(3), 375–386.

Zhang, F., & Yeh, A. G. O. (2011). Editorial: sustainable urban development. *Computers, Environment and Urban Systems, 35*, 345–346.

Zhang, J. Q., & Wang, Y. P. (2008). Study of the relationships between the spatial extent of surface urban heat islands and urban characteristic factors based on Landsat ETM plus data. *Sensors, 8*, 7453–7468.